Chinese Physics Letters

LETTER

From Topological Order to Mixed-State Phases: A Ground-State Probe of Fractionalized Excitations

Cite as: Yunlong Zang *et al*. 2026 *Chin. Phys. Lett.* **43** 100701

DOI CSTR

Recommended Articles

Diagnosing 2D Symmetry Protected Topological States Via Mixed State Anomaly
Chao Xu, Yunlong Zang, Yixin Ma, Yingfei Gu, and Shenghan Jiang
Chin. Phys. Lett. **43**, 080704 (2026)

Ground State and Its Topological Properties of Three-Dimensional Spin-Orbit Coupled Degenerate Fermi Gases
Long Xiong, Ming Gong, Zhao-Xiang Fang, and Rui Sun
Chin. Phys. Lett. **40**, (2023)

Symmetric Mass Generation Transition and its Nonequilibrium Critical Dynamics in a Bilayer Honeycomb Lattice Model
Zhi-Xuan Li, Yin-Kai Yu, Zi-Xiang Li, and Shuai Yin
Chin. Phys. Lett. , (2026)

Decoding Equilibrium and Dynamical Criticality in the 2D Topological Order
Xiao-Ming Zhao, Cui-Xian Guo, Gaoyong Sun, and Su-Peng Kou
Chin. Phys. Lett. **43**, 070707 (2026)

A series journal of Chinese Physical Society distributed by IOP Publishing

Chinese Physics Letters

Chin. Phys. Lett. **43** 100701 (2026)

LETTER

DOI: 10.1088/0256-307X/43/10/100701
CSTR: 32039.14.0256-307X.43.10.100701

From Topological Order to Mixed-State Phases: A Ground-State Probe of Fractionalized Excitations

Yunlong Zang†, Yu-Bin Li†, and Shenghan Jiang*

Kavli Institute for Theoretical Sciences and School of Quantum, University of Chinese Academy of Sciences, Beijing 100190, China

†These authors contributed equally to this work.
*Corresponding author. Email: jiangsh@ucas.ac.cn

How do we detect topological phases from a single ground state? Entanglement entropy and spectrum have long been the standard tools—but the reduced density matrix (RDM) itself contains far more information. We show that the RDM of a 2D topologically ordered system, expressed at the entanglement cut, realizes a 1D mixed-state phase. For the $\mathbb{Z}_2$ toric code phase, it is a 1D $\mathbb{Z}_2$ strong-to-weak spontaneous symmetry breaking (SW-SSB) phase, where deconfinement of anyons manifests as the short-range correlation of both $\mathbb{Z}_2$ charge and $\mathbb{Z}_2$ domain-wall in the RDM. The bulk *e*–*m* duality translates into a Kramers–Wannier self-duality of the SW-SSB phase. Extending the framework to gapped $\mathbb{Z}_2$ spin liquids, the global spin-rotation symmetry manifests as an additional weak symmetry for the 1D RDM. Spin-1/2 spinons result in a cusp on the disorder parameter of spin-rotation at $\theta = \pi$, providing a direct, ground-state signature of symmetry fractionalization. We verify this prediction analytically using the matrix product density operator formalism and numerically for the kagome-lattice resonating valence bond state. The proposed observable requires only a single ground-state wavefunction, making it amenable to quantum simulation platforms.

Introduction

Topologically ordered phases, characterized by long-range entanglement and anyonic excitations, stand as a cornerstone of modern condensed matter physics [1–4]. While routinely identified by global signatures such as ground-state degeneracy on the torus [5], their experimental detection remains a formidable challenge—one that demands new theoretical tools beyond conventional order parameters.

Entanglement-based diagnostics have partially filled this gap. The topological entanglement entropy—a universal subleading constant in the area law—quantifies the total quantum dimension of anyons [6,7]. The entanglement spectrum mimics edge-mode dispersions, particularly for chiral phases [8]. These measures are derived from the reduced density matrix (RDM), suggesting that the RDM itself should encode richer information about the underlying topological order [9,10].

The key insight of this work is that the RDM of a 2D topological phase, evaluated at the entanglement cut, realizes a nontrivial 1D mixed state phase [11–19]. This pure–mixed correspondence—recently explored from complementary perspectives [20–26]—opens a new window into topological order through the lens of mixed-state phases. Specifically, for the $\mathbb{Z}_2$ toric code topological order, we demonstrate that its RDM realizes a 1D $\mathbb{Z}_2$ strong-to-weak spontaneous symmetry breaking (SW-SSB) phase [13,18,27–33], in which a strong symmetry ($\rho = U\rho = \rho U$) [11,34] is spontaneously broken to a weak one ($\rho = U\rho U^\dagger$). Here, the strong $\mathbb{Z}_2$ symmetry inherited from the bulk one-form symmetry [35,36] is spontaneously broken to a weak one, and this SW-SSB directly signals the deconfinement of anyons.

This correspondence is powerful in two complementary ways. First, it inspires a definition of 1D SW-SSB phases based solely on linear correlators: the charged-operator correlator and the domain-wall correlator [37,38] both decay exponentially, manifesting the deconfinement of *e* and *m* anyons [39]. The bulk *e*–*m* electromagnetic duality translates into the Kramers–Wannier (KW) self-duality of 1D SW-SSB phase [40,41]. Second, the framework, when extended to gapped $\mathbb{Z}_2$ spin liquids [13,42–45], leads to a powerful new method for detecting symmetry fractionalization [46–48]. We prove analytically—using a matrix product density operator (MPDO) description of the 1D RDM—that the spin-rotation disorder parameter $\langle U_A(\theta)\rangle$ [49–58] develops a non-analytic cusp at rotation angle $\theta = \pi$ when *e*-anyon carries spin-1/2. We verify this prediction numerically using the nearest-neighbor resonating valence bond (NN-RVB) state on the kagome lattice. This provides a direct, ground-state probe of spinons that requires only a single wavefunction, which is readily implementable on quantum simulation platforms.

RDM of the Toric Code Phase

We start by deriving the RDM as a 1D mixed state for the toric code model on a square lattice [59]. As shown in Fig. 1, the system is partitioned into two simply connected regions, A and $\bar{A}$, with cut length L. The toric code Hamiltonian naturally decomposes as

$$H = -\sum_p \prod_{i\in p} Z_i - \sum_v \prod_{i\in v} X_i \equiv H_A + H_{\bar{A}} + H_{\partial A\cup\partial\bar{A}}, \tag{1}$$

where H_A and $H_{\bar{A}}$ contain all local terms entirely within A and $\bar{A}$, respectively, and $H_{\partial A\cup\partial\bar{A}}$ consists of the $2L$ stabilizer terms that intersect the entanglement cut (colored dots in Fig. 1).

As all local terms commute, ground states of H are the simultaneous ground states of all three parts. We first examine the ground state subspace of H_A, denoted as $\mathcal{H}_{\partial A}$. At first glance, $\mathcal{H}_{\partial A}$ contains L local zero-modes at ∂A, described by L pairs of Pauli operators commuting with H_A:

$$\tau^x_k \equiv X^A_{2k}, \quad \tau^z_k\tau^z_{k+1} \equiv Z^A_{2k}Z^A_{2k+1}Z^A_{2k+2}, \tag{2}$$

where X^A_j/Z^A_j act on the jth red-colored qubit in Fig. 1. Here, τ^x_k creates a pair of domain walls at $k\pm 1/2$, which is identified as two m-anyons, and τ^z_k creates $\mathbb{Z}_2$ charge at k, identified as e-anyon. Note that the relation $\hat{1} = \prod_k \tau^z_k\tau^z_{k+1} = \prod_k Z^A_{2k+1}$ is not an operator identity—rather, it holds within the ground-state subspace $\mathcal{H}_{\partial A}$: $\prod_k Z^A_{2k+1} = \prod_{p\in A}\prod_{i\in p} Z_i$ measures the total m-anyon parity in A, which vanishes in $\mathcal{H}_{\partial A}$. Further, a closer analysis reveals that there are only $(L-1)$

Received 14 July 2026; accepted 28 August 2026; published 2 November 2026

© 2026 Chinese Physical Society and IOP Publishing Ltd. All rights, including for text and data mining, AI training, and similar technologies, are reserved.

Check for updates

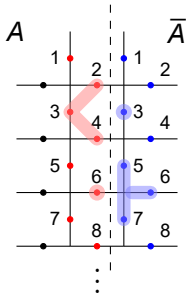

Fig. 1. Bipartition of the toric code model on a square lattice. Qubits at ∂A ($\partial\bar{A}$) are denoted by red (blue) dots. Regions A and $\bar{A}$ are simply connected; the zoomed view shows qubit indices along the entanglement cut.

independent zero-modes. This reduction stems from the constraint where the number of e-anyon equals 0 in $\mathcal{H}_{\partial A}$,

$$\prod_{k=1}^{L}\tau_k^x=\prod_{v\in A}\prod_{i\in v}X_i=\hat{1}. \tag{3}$$

Therefore, $\mathcal{H}_{\partial A}$ can be viewed as a 1D qubit chain of length L subject to a $\mathbb{Z}_2$ global constraint in Eq. (3).

Similarly, the ground subspace $\mathcal{H}_{\partial\bar{A}}$ also describes a 1D qubit chain, with corresponding Pauli operators

$$\bar{\tau}_k^x\equiv X_{2k-1}^{\bar{A}}X_{2k}^{\bar{A}}X_{2k+1}^{\bar{A}},\quad \bar{\tau}_k^z\bar{\tau}_{k+1}^z\equiv Z_{2k+1}^{\bar{A}}, \tag{4}$$

where $X_j^{\bar{A}}$ and $Z_j^{\bar{A}}$ act on the jth blue-colored qubit in Fig. 1. The L local qubits obey the global $\mathbb{Z}_2$ constraint $\prod_{k=1}^{L}\bar{\tau}_k^x=\hat{1}$, indicating zero e-anyon inside $\bar{A}$ within $\mathcal{H}_{\bar{A}}$. In addition, the identity $\hat{1}=\prod_{k=1}^{L}\bar{\tau}_k^z\bar{\tau}_{k+1}^z=\prod_k Z_{2k+1}^{\bar{A}}$ holds in $\mathcal{H}_{\partial\bar{A}}$, indicating zero m-anyon.

The ground states of the full H are now obtained by solving ground states of $H_{\partial A\cup\partial\bar{A}}$ within $\mathcal{H}_{\partial A}\otimes\mathcal{H}_{\partial\bar{A}}$. In terms of τ_A and $\tau_{\bar{A}}$, $H_{\partial A\cup\partial\bar{A}}$ takes form

$$H_{\partial A\cup\partial\bar{A}}=-\sum_{k=1}^{L}(\tau_k^x\bar{\tau}_k^x+\tau_k^z\tau_{k+1}^z\bar{\tau}_k^z\bar{\tau}_{k+1}^z), \tag{5}$$

subject to the global $\mathbb{Z}_2\times\mathbb{Z}_2$ constraint $\prod_k\tau_k^x=\prod_k\bar{\tau}_k^x=\hat{1}$. Its ground state $|\psi\rangle$ is completely determined by minimizing all local terms in Eq. (5), together with the $\mathbb{Z}_2\times\mathbb{Z}_2$ constraint. Tracing out $\tau_{\bar{A}}$ yields RDM for region A, expressed in the τ basis. This RDM, denoted $\rho_{\partial A}$, satisfies the local constraints

$$[\tau_k^x,\rho_{\partial A}]=[\tau_k^z\tau_{k+1}^z,\rho_{\partial A}]=0, \tag{6}$$

as well as a $\mathbb{Z}_2$ strong symmetry due to the global constraint of $\mathcal{H}_{\partial A}$:

$$\rho_{\partial A}=\prod_{k=1}^{L}\tau_k^x\cdot\rho_{\partial A}=\rho_{\partial A}\cdot\prod_{k=1}^{L}\tau_k^x. \tag{7}$$

These constraints lead to a unique solution

$$\rho_{\partial A}=\frac{1}{2^L}\left(\hat{1}+\prod_k\tau_k^x\right). \tag{8}$$

The above procedure to express RDM ρ_A as a 1D mixed state $\rho_{\partial A}$ generalized readily to $\mathbb{Z}_2$ topological ordered systems beyond the exact solvable point. We sketch the generalization here, and provide a more rigorous derivation using the framework of projected entangled pair states (PEPS) in Section I of the Supplementary Materials (SM).

The full system can be decomposed as $H_A+H_{\bar{A}}+H_{\partial A\cap\partial\bar{A}}$, where $H_{\partial A\cap\partial\bar{A}}$ contains all terms localized within a correlation length ξ of the entanglement cut. To construct the ground state, we first solve low-energy subspaces $\mathcal{H}_{\partial A}$ and $\mathcal{H}_{\partial\bar{A}}$ of regions A and $\bar{A}$. As in the exact solvable case, $\mathcal{H}_{\partial A}$ supports anyonic excitations near the cut, and is effectively described by a 1D $\mathbb{Z}_2$ Ising chain. Here, the e-anyon corresponds to a $\mathbb{Z}_2$ charge τ^z, and the m-anyon corresponds to a $\mathbb{Z}_2$ domain wall—an endpoint of a τ^x-string. While we use Pauli notation $\tau^{x,z}$ for clarity, the essential structure for a generic model is that the effective boundary operators satisfy the Pauli algebra: $(\tau^z)^2=(\tau^x)^2=\hat{1}$ encodes the $\mathbb{Z}_2$ fusion rules of e and m, while $\{\tau^x,\tau^z\}=0$ reflects their semionic mutual statistics.

The absence of excitations in region A imposes constraints on $\mathcal{H}_{\partial A}$: the m-loop and e-loop operators along the cut must act as identity in $\mathcal{H}_{\partial A}$. Expressed in terms of the effective $\mathbb{Z}_2$ Ising variables near the cut, the m-loop constraint imposes periodic boundary condition (PBC), and the e-loop constraint restricts $\mathcal{H}_{\partial A}$ within the $\mathbb{Z}_2$ even sector $\prod_j\tau_j^x=\hat{1}$. An analogous description applies for $\mathcal{H}_{\partial\bar{A}}$.

When restricted to $\mathcal{H}_{\partial A}\otimes\mathcal{H}_{\partial\bar{A}}$, the full ground state $|\Psi\rangle$ is approximated by the ground state $|\psi\rangle$ of $H_{\partial A\cap\partial\bar{A}}$. Since the full system is in a uniform topological phase, anyons can traverse the entanglement cut. This is realized by condensing bound pairs of e- and m-anyons that bridge the two sides of the cut, while leaving individual anyons deconfined. Translating to the Ising chain language, this implies condensing $\tau^z\bar{\tau}^z$ and proliferating the $\tau^x\bar{\tau}^x$-string,

$$\langle\tau_i^z\bar{\tau}_i^z\tau_j^z\bar{\tau}_j^z\rangle\xrightarrow{|i-j|\to\infty}C_e,\quad\left\langle\prod_{k=i}^{j}\tau_k^x\bar{\tau}_k^x\right\rangle\xrightarrow{|i-j|\to\infty}C_m. \tag{9}$$

The long-range correlation of $\tau^z\bar{\tau}^z$ (creates $\mathbb{Z}_2\times\mathbb{Z}_2$ charge) signals that the $\mathbb{Z}_2\times\mathbb{Z}_2$ symmetry is spontaneously broken to some subgroup, while the non-decaying $\tau^x\bar{\tau}^x$-string (creates diagonal $\mathbb{Z}_2$ domain walls) confirms that the diagonal $\mathbb{Z}_2$ subgroup remains unbroken. Hence, $|\psi\rangle$ realizes a $\mathbb{Z}_2\times\mathbb{Z}_2\to\mathbb{Z}_2$ SSB phase.

Tracing out $\mathcal{H}_{\partial\bar{A}}$ yields the 1D mixed state $\rho_{\partial A}$, which holds a $\mathbb{Z}_2$ strong symmetry $\prod_k\tau_k^x$. The SSB pattern of $|\psi\rangle$ translates into the simultaneous exponential decay of both the diagonal $\mathbb{Z}_2$ charged-operator correlator and the off-diagonal $\mathbb{Z}_2$ domain walls,

$$\mathrm{Tr}(\rho_{\partial A}\tau_i^z\tau_j^z)\sim\mathrm{e}^{-|i-j|/\xi_e},\quad\mathrm{Tr}\left(\rho_{\partial A}\prod_{k=i}^{j}\tau_k^x\right)\sim\mathrm{e}^{-|i-j|/\xi_m}. \tag{10}$$

In terms of anyons, equation (10) is interpreted as neither e nor m is condensed, and ξ_e and ξ_m are the correlation lengths of e and m anyons, respectively. In the exact solvable limit, these correlators vanish strictly due to Eq. (6).

The 1D SW-SSB Phase

In summary, the 1D RDM $\rho_{\partial A}$ of a generic $\mathbb{Z}_2$ topological ordered state exhibits the following universal properties:

1. $\mathbb{Z}_2$ strong symmetry, indicating zero e;
2. PBC, signaling zero m;
3. Exponential decay of both $\mathbb{Z}_2$ charge and $\mathbb{Z}_2$ domain-wall correlators [Eq. (10)], signaling anyon deconfinement.

Notably, property 3 cannot occur in any pure ground state(s) of a $\mathbb{Z}_2$ symmetric Ising chains [38].

We define the 1D strong $\mathbb{Z}_2$ symmetric $\rho_{\partial A}$ whose correlation function satisfies Eq. (10) as the SW-SSB mixed-state phase. Physically, the exponential decay of $\mathbb{Z}_2$ domain wall operators signals that the strong $\mathbb{Z}_2$ symmetry is broken. Meanwhile, operator τ^z carries charge under the induced $\mathbb{Z}_2$ weak symmetry (the diagonal subgroup of $\mathbb{Z}_2\times\mathbb{Z}_2$); hence, the exponential decay of $\langle\tau_i^z\tau_j^z\rangle$ indicates that the $\mathbb{Z}_2$ weak symmetry remains unbroken. Our definition of SW-SSB—based solely on linear observables in $\rho_{\partial A}$—is distinct from characterizations via fidelity correlators [18] or Wightman functions [29,30] involving $\sqrt{\rho}$. Such linear observables are directly accessible in experiments and numerical simulations, whereas extracting $\sqrt{\rho}$ in general requires full state tomography. A detailed comparison between these approaches is provided in Section II of the SM.

A remarkable consequence of this definition is that the 1D $\mathbb{Z}_2$ SW-SSB phase with PBC is self-dual under the KW transformation. Physically, KW duality exchanges the $\mathbb{Z}_2$ charge with the $\mathbb{Z}_2$ domain-wall,

$$\tau^z_k\tau^z_{k+1} \to \tau^x_{k+1}, \quad \tau^x_k \to \tau^z_k\tau^z_{k+1}. \tag{11}$$

For a mixed-state satisfying Eq. (10), the KW transformation simply interchanges ξ_e and ξ_m, preserving the short-range character of both correlators. Globally, the KW transformation maps the even-$\mathbb{Z}_2$-charge condition $\prod_k \tau^x_k = 1$ ($\mathbb{Z}_2$ strong symmetry) to the even-domain-wall condition $\prod_k \tau^z_k\tau^z_{k+1} = 1$ (PBC $\tau^z_{L+1} \equiv \tau^z_1$). Consequently, a mixed state $\rho_{\partial A}$ in the 1D $\mathbb{Z}_2$ SW-SSB phase with PBC is self-dual. Such self-duality has a natural bulk interpretation: it reflects the $e \leftrightarrow m$ electromagnetic duality of the toric code (see details in Section III of the SM).

The pure–mixed correspondence extends to all three phases of $\mathbb{Z}_2$ gauge theory [60], completing the dictionary:

- **Deconfined phase** $\longleftrightarrow$ **SW-SSB phase**: both the charged-operator and domain-wall correlators decay exponentially [Eq. (10)].
- **Confined phase** (m condenses) $\longleftrightarrow$ **symmetric phase**: domain walls proliferate while the charged correlator decays.
- **Higgs phase** (e condenses) $\longleftrightarrow$ **SSB phase**: the $\mathbb{Z}_2$ charge condenses and long-range ordered while the domain wall decays; the strong symmetry is fully broken.

This three-way correspondence was first proposed in the PEPS context by Ref. [61], where the 1D boundary matrix product state fixed points of the deformed toric code PEPS were discussed. We provide a detailed derivation and numerical verification in Sections I and IV of the SM.

Application: Detecting Symmetry Fractionalization

The pure–mixed correspondence between 2D topological phases and 1D mixed-state phases is more than a formal mapping—it provides a practical framework for extracting universal observables directly from a single ground state wavefunction. Here, we generalize this framework to gapped $\mathbb{Z}_2$ spin liquids with global spin-rotation symmetry, where the e-anyon carries spin-1/2, identified as the fractionalized spinon. The crucial new ingredient is the global spin-rotation symmetry, which manifests as a weak symmetry of the 1D mixed state $\rho_{\partial A}$—in contrast to the $\mathbb{Z}_2$ strong symmetry that encodes the topological order. A classic example is the NN-RVB state [42] on a frustrated spin-1/2 system [42].

While spinons are typically probed through the dynamic spin structure factor [62]—where they produce a low-energy continuum instead of sharp spin-wave peaks—this spectral feature is often obscured by impurities experimentally [45]. Our approach offers a ground-state alternative: we propose that the presence of gapped spinon spectrum can be detected through the spin rotation disorder parameter $|\langle U_A(\theta)\rangle|$ in a large subregion A, where

$$|\langle U_A(\theta)\rangle| \equiv |\mathrm{Tr}[\rho_A U_A(\theta)]|, \quad U_A(\theta) = \prod_{j\in A} \exp(\mathrm{i}\theta S^z_j). \tag{12}$$

In symmetric phases, it obeys an area law [37], where $|\langle U_A(\theta)\rangle| \sim \mathrm{e}^{-f(\theta)L}$, for some function $f(\theta)$. Crucially, when the e-anyon carries half-integer spin, $f(\theta)$ develops non-smooth behavior as a function of θ. Numerical evidence supporting this prediction, obtained from NN-RVB state on the kagome lattice, is presented in Fig. 2 (details are given in Section IV of the SM).

The above result can be derived analytically using the MPDO formalism. The logic of the derivation is as follows. We encode $\rho_{\partial A}$ as an MPDO and impose the $\mathbb{Z}_2$ SW-SSB and $U(1)$ symmetry conditions as constraints on the local tensor M. The disorder parameter $\langle U_A(\theta)\rangle$, when evaluated in the thermodynamic limit, equals the dominant eigenvalue of a θ-twisted transfer matrix $T(\theta)$. The symmetry fractionalization condition forces an eigenvalue crossing between $\theta = 0$ and $\theta = 2\pi$, and the Hermiticity of $\rho_{\partial A}$ further pins the crossing to $\theta = \pi$. The detailed derivation follows.

As in the case of pure $\mathbb{Z}_2$ topological order, $\rho_{\partial A}$ of a gapped $\mathbb{Z}_2$ spin liquid also belongs to the $\mathbb{Z}_2$ SW-SSB phase: it possesses a strong $\mathbb{Z}_2$ symmetry generated by the m-anyon loop, denoted as $J_{\partial A}$

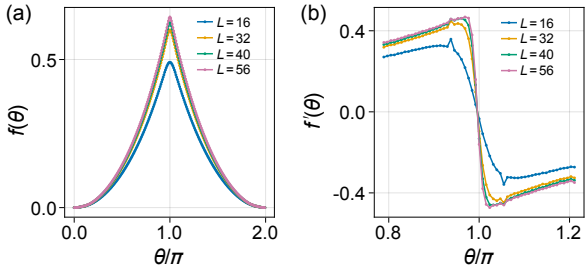

Fig. 2. Disorder parameters of the NN-RVB state on the kagome lattice. The non-smoothness at $\theta = \pi$ corresponds to a discontinuity in the derivative $f'(\theta)$. The large-L behavior of this discontinuity can be approximated using Eq. (28).

[Eq. (7)], and exhibits short-range correlation condition in Eq. (10). The key new ingredient for spin liquids is the incorporation of global spin rotation symmetry $U(\theta) = \mathrm{e}^{\mathrm{i}S^z\theta}$. This global symmetry manifests as a weak $U(1)$ symmetry on RDM ρ_A. Denoting its representation in the entanglement space as $W_{\partial A}(\theta) = \prod_{j\in A} W_j(\theta)$, we have $[\rho_{\partial A}, W_{\partial A}(\theta)] = 0$. For the NN-RVB case, the e-anyon carries half-integer spin, identified as the spinon. Therefore, $W_{\partial A}(2\pi) \circ e = -e$, identifying it as the m-anyon loop,

$$W_{\partial A}(2\pi) = J_{\partial A}. \tag{13}$$

With these properties in place, we make a further simplifying assumption: the 1D mixed state $\rho_{\partial A}$ is well approximated by an MPDO,

$\rho_{\partial A} = \mathrm{Tr}[M^{L_{\partial A}}] =$ 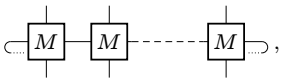 , (14)

where M denotes the local tensor of the MPDO. Hence, the disorder parameter reads

$\langle U_A(\theta)\rangle = \mathrm{Tr}(\rho_{\partial A}\cdot W_{\partial A}(\theta)) = \mathrm{Tr}(T(\theta)^L)$

$=$ 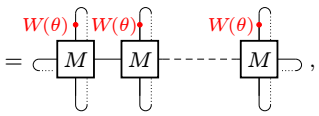 , (15)

where the θ-twisted transfer matrix is

$T(\theta) =$ 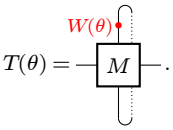 .

In the thermodynamic limit, we have

$$f(\theta) \xrightarrow{L\to\infty} -\log|\alpha_{\max}(\theta)|, \tag{16}$$

where $\alpha_{\max}(\theta)$ is the eigenvalue of $T(\theta)$ with the largest modulus.

To proceed, we implement the symmetry of $\rho_{\partial A}$ on the MPDO, which manifests as gauge transformation on virtual legs of local tensor M. First, the $\mathbb{Z}_2$ strong symmetry $\rho_{\partial A} = J_{\partial A}\cdot\rho = \rho\cdot J_{\partial A}$ leads to

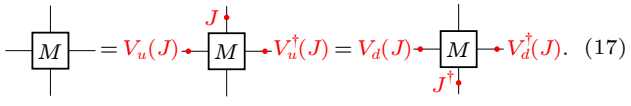

(17)

Physically, $V_u(J)$ or $V_d(J)$ creates an m-anyon in the ket or bra layer. To capture the $\mathbb{Z}_2$ SW-SSB for $\rho_{\partial A}$ in MPDO, a virtual leg $\mathbb{Z}_2$ symmetry is introduced (see Section V of the SM for more details),

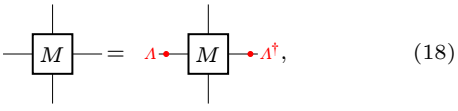

(18)

where $\Lambda^2 = \hat{1}$, and

$$\Lambda \cdot V_{u/d}(J) = -V_{u/d}(J) \cdot \Lambda. \tag{19}$$

Physically, Λ creates e-anyon at both bra and ket spaces, and its anticommutation with $V_{u/d}(J)$ in Eq. (19) reflects the mutual semionic statistics between e and m. As shown in section V of the SM, imposing Eqs. (17) and (18) immediately imply the exponential decay of both charge and domain walls.

Now, imposing the global $U(1)$ spin rotation symmetry, which further constrains M as

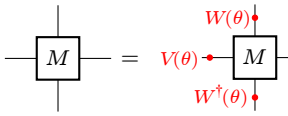

(20)

The algebraic relations for gauge transformation V's follow those on physical legs of the MPDO. In particular, $V(2\pi) = V_u(J)V_d(J)$ due to Eq. (13).

Symmetries of θ-twisted transfer matrix can be derived from the above equations as

$$T(\theta) = \Lambda \cdot T(\theta) \cdot \Lambda^\dagger = V(\theta') \cdot T(\theta) \cdot V^\dagger(\theta') \tag{21}$$

for any angle θ'.

Equipped with these symmetry properties, we now investigate the flow of the dominant eigenvalue for $T(\theta)$, which determines the behavior of disorder parameter $f(\theta)$. When $\theta = 0$, the transfer matrix $T(0)$ holds non-degenerate dominant eigenvalue. Let $|r_1(0)\rangle$ be the leading eigenvector of $T(0)$ with eigenvalue $\alpha_0(0)$. We track the smooth trajectory of $\alpha_0(\theta)$ starting from $\theta = 0$ to $\theta = 2\pi$,

$$T(\theta)|r_0(\theta)\rangle = \alpha_0(\theta)|r_0(\theta)\rangle, \tag{22}$$

where $\alpha_0(\theta)$ and $|r_0(\theta)\rangle$ are smooth.

Due to the fractionalized spinon feature where $W(2\pi) = J$ [Eq. (13)], $T(\theta + 2\pi)$ are then related to $T(\theta)$ by a gauge transformation,

$$T(\theta + 2\pi) = V_u^\dagger(J) \cdot T(\theta) \cdot V_u(J). \tag{23}$$

Therefore, $V_u^\dagger(J)|r_0(0)\rangle$ is then non-degenerate dominant eigenvector of $T(2\pi)$, where

$$T(2\pi) \cdot V_u^\dagger(J)|r_0(0)\rangle = \alpha_0(0) \cdot V_u^\dagger(J)|r_0(0)\rangle. \tag{24}$$

Comparing with Eq. (22), one might identify $V_u^\dagger(J)|r_0(0)\rangle$ with $|r_0(2\pi)\rangle$. However, we will show that these two states are distinct. The continuity of $|r_0(\theta)\rangle$ implies that $|r_0(2\pi)\rangle$ and $|r_0(0)\rangle$ share the same quantum number under symmetry Λ. However, due to the anticommutation relation in Eq. (19), $V_u^\dagger(J)|r_0(0)\rangle$ hosts opposite quantum number under Λ from $|r_0(0)\rangle$. Therefore, we conclude that $|\alpha_0(2\pi)| < |\alpha_{\max}(2\pi)| = |\alpha_0(0)|$, and the exchange of the dominant eigenvalue in general leads to the non-smooth $f(\theta)$ due to Eq. (16), consistent with Fig. 2.

We note that there is another key feature in Fig. 2(a), where the non-smooth point is at $\theta = \pi$. In terms of $T(\theta)$, such behavior means that the largest two eigenvalues of $T(2\pi)$ crosses at $\theta = \pi$, and is degenerate. To analytically derive this, we further consider the Hermiticity condition $\rho = \rho^\dagger$, which imposes local tensor constraints

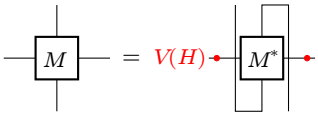

(25)

where $[V(H)\mathcal{K}]^2 = \hat{1}$ and $V(H)\mathcal{K} \cdot V_u(J) = V_d(J) \cdot V(H)\mathcal{K}$, with $\mathcal{K}$ complex conjugation. Hence,

$$T(\theta) = V(H) \cdot T^*(-\theta) \cdot V^\dagger(H). \tag{26}$$

Together with Eq. (23), we conclude

$$T(\pi) = V(H)\mathcal{K}V_u(J) \cdot T(\pi) \cdot [V(H)\mathcal{K}V_u(J)]^\dagger. \tag{27}$$

From Eq. (19), $\{V(H)\mathcal{K}V_u(J), \Lambda\} = 0$. Hence, $|\alpha_0(\pi)\rangle$ and $V(H)\mathcal{K}V_u(J)|\alpha_0(\pi)\rangle$ are distinct eigenstates of $T(\pi)$ with complex-conjugate eigenvalues, as they have different quantum numbers under Λ. This explains the non-smoothness at $\theta = \pi$ in Fig. 2(a). Moreover, the finite-size rounding of the discontinuity can also be derived from this level-crossing feature. As detailed in Section IV.C of the SM, the symmetry and Hermiticity of $T(\theta)$ further constrain the two dominant branches to form a complex-conjugate pair at $\theta = \pi$, $\alpha_1(\pi) = \alpha_2^*(\pi)$, with opposite slopes of their moduli, $f_1'(\pi) = -f_2'(\pi)$, where $f_i \equiv \ln|\alpha_i|$. For $\theta = \pi + \delta$ and large but finite L, one finds

$$f_L'(\pi + \delta) \simeq -f_1'(\pi) \frac{\sinh\left(2Lf_1'(\pi)\delta\right)}{\cosh\left(2Lf_1'(\pi)\delta\right) + \cos\left(2L\varphi_1\right)}, \tag{28}$$

with $\varphi_1 \equiv \arg\alpha_1(\pi)$. Hence, at any finite L, $f'(\pi) = 0$ and the cusp is smoothly rounded over a window $|\delta| \sim 1/L$, while a discontinuity of magnitude $2\left|f_1'(\pi)\right|$ develops as $L \to \infty$.

As a further application of this framework, the MPDO analysis can be extended to other SET phases. In Section VI of the SM, we show that for a $\mathbb{Z}_2$ SET where the e-anyon carries a fractional $\mathbb{Z}_2$ quantum number, the m-anyon correlator in the presence of a $\mathbb{Z}_2$ disorder operator becomes long-range ordered,

$$\frac{\langle m_i m_j U_A(g)\rangle}{\langle U_A(g)\rangle} \xrightarrow{|i-j|\to\infty} O(1), \tag{29}$$

with i and j located near ∂A.

Summary and Discussion

The central message of this work is that the RDM of a 2D topological phase, evaluated at an entanglement cut, realizes a 1D nontrivial mixed-state phase, whose symmetry and correlation structure directly encodes universal topological data. For the $\mathbb{Z}_2$ toric code, the RDM at the entanglement cut realizes a 1D $\mathbb{Z}_2$ SW-SSB phase, whose self-duality under the KW transformation reflects the electromagnetic duality of the bulk topological order. By extending this framework to gapped $\mathbb{Z}_2$ spin liquids, we propose a direct ground-state diagnostic of spin-rotation symmetry fractionalization, where the corresponding disorder parameter develops a non-analytic cusp at $\theta = \pi$. Analytical derivations based on MPDO and numerical results for the kagome-lattice RVB state are provided to corroborate this prediction.

Several comments are in order on the generality of our diagnostic with respect to other anyon species and other types of symmetry. First, since $f = e \times m$, its symmetry fractionalization pattern is fully determined by those of e and m; it is therefore sufficient to consider the latter two. Second, although we have focused on fractional charge carried by the e-anyon, the e–m duality implies that symmetry fractionalization of the m-anyon produces a similar non-analytic behavior of the disorder parameter. Finally, for spatial symmetries, the disorder operator—a lattice operation applied to a subregion A—is difficult to implement experimentally, and detecting spatial symmetry fractionalization in a single ground state calls for other diagnostics.

Looking forward, our work suggests several promising directions. The linear-correlator definition of the SW-SSB phase readily generalizes to d-dimensional mixed states with a strong n-form symmetry [63]. In this case, both the order parameter $\langle O_c\rangle$ (supported on a closed n-dimensional manifold M_c) and the disorder parameter $\langle O_d\rangle$ [supported on a $(d-n)$-dimensional manifold with boundary M_d] obey "volume-law" scaling,

$$-\ln|\langle O_c\rangle| \propto V_{n+1}^c, \quad -\ln|\langle O_d\rangle| \propto V_{d-n}^d, \tag{30}$$

where V_{n+1}^c is the minimal volume of manifolds bounded by M_c, and V_{d-n}^d is the volume of M_d.

The natural extension of the pure–mixed correspondence to topological phases with non-invertible (categorical) symmetries [36,64] is particularly compelling, as the framework may shed new light on detection of such exotic orders. Extending these ideas to chiral topological phases remains an important open problem.

Two more general situations of detecting SET phases lie beyond the scope of the present work. First, when e and m are both fractionalized under the same symmetry, the $\mathbb{Z}_2$ SW-SSB representation of the RDM is no longer sufficient, and one needs other isomorphic maps from the 2D RDM to 1D mixed-state phases beyond this paradigm. Note that, much like the bulk–boundary correspondence, the choice of the 1D mixed-state representation of a given 2D RDM is in general not unique. Second, there exist SET orders beyond symmetry fractionalization, such as symmetries exchanging anyons; capturing and detecting such orders also requires a framework beyond this work.

The most immediate implication of this work is experimental: the disorder parameter $\langle U_A(\theta)\rangle$ is a concrete, measurable observable that can be accessed on quantum simulation platforms. It requires only a single ground-state wavefunction, making it a practical route to detecting signatures of fractionalized excitations in engineered quantum systems.

Acknowledgment

We thank Pengfei Zhang, Yingfei Gu, Meng Cheng, and Yunqin Zheng for helpful discussions. This work was supported by the Ministry of Science and Technology of China (Grant No. 2022YFA1403902) and the National Natural Science Foundation of China (Grant No. 12574179).

References

[1] Wen X G 1990 *Int. J. Mod. Phys. B* **4** 239
[2] Kitaev A Y 2003 *Ann. Phys.* **303** 2
[3] Kitaev A 2006 *Ann. Phys.* **31** 2
[4] Wen X G 2017 *Rev. Mod. Phys.* **89** 041004
[5] Wen X G and Niu Q 1990 *Phys. Rev. B* **41** 9377
[6] Kitaev A and Preskill J 2006 *Phys. Rev. Lett.* **96** 110404
[7] Levin M and Wen X G 2006 *Phys. Rev. Lett.* **96** 110405
[8] Li H and Haldane F D M 2008 *Phys. Rev. Lett.* **101** 010504
[9] Cirac J I, Poilblanc D, Schuch N, and Verstraete F 2011 *Phys. Rev. B* **83** 245134
[10] Schuch N, Poilblanc D, Cirac J I, and Pérez-García D 2013 *Phys. Rev. Lett.* **111** 090501
[11] de Groot C, Turzillo A, and Schuch N 2022 *Quantum* **6** 856
[12] Ma R and Wang C 2023 *Phys. Rev. X* **13** 031016
[13] Lee J Y, Jian C M, and Xu C 2023 *PRX Quantum* **4** 030317
[14] Chen Y H and Grover T 2024 *PRX Quantum* **5** 030310
[15] Sang S, Zou Y, and Hsieh T H 2024 *Phys. Rev. X* **14** 031044
[16] Ma R and Turzillo A 2025 *PRX Quantum* **6** 010348
[17] Ma R, Zhang J H, Bi Z, Cheng M, and Wang C 2025 *Phys. Rev. X* **15** 021062
[18] Lessa L A, Ma R, Zhang J H, Bi Z, Cheng M, and Wang C 2025 *PRX Quantum* **6** 010344
[19] Sang S, Lessa L A, Mong R S K, Grover T, Wang C, and Hsieh T H 2025 arXiv:2507.02292 [quant-ph]
[20] Luo R, Wang Y N, and Bi Z 2025 *PRX Quantum* **6** 040358
[21] Schafer-Nameki S, Tiwari A, Warman A, and Zhang C 2025 arXiv:2507.05350 [quant-ph]
[22] Qi M, Sohal R, Chen X, Stephen D T, and Prem A 2025 arXiv:2507.05335 [cond-mat.str-el]
[23] Lu T C, Liu Y J, Gopalakrishnan S, and You Y 2025 arXiv:2511.19597 [quant-ph]
[24] Sala P, Pollmann F, Oshikawa M, and You Y 2026 *Quantum Sci. Technol.* **11** 025017
[25] Xu C, Zang Y, Ma Y, Gu Y, and Jiang S 2025 arXiv:2506.13096 [cond-mat.str-el]
[26] Ma Y, Xu C, and Jiang S 2025 arXiv:2511.10163 [cond-mat.str-el]
[27] Sala P, Gopalakrishnan S, Oshikawa M, and You Y 2024 *Phys. Rev. B* **110** 155150
[28] Lu S, Zhu P, and Lu Y M 2024 arXiv:2411.07174 [cond-mat.str-el]
[29] Liu Z, Chen L, Zhang Y, Zhou S, and Zhang P 2025 *Commun. Phys.* **8** 274
[30] Weinstein Z 2025 *Phys. Rev. Lett.* **134** 150405
[31] Divi F, Lessa L A, and Wang C 2026 arXiv:2605.28967 [quant-ph]
[32] Zhang C 2026 arXiv:2605.29113 [quant-ph]
[33] Liu R, Yi J, and Else D V 2026 arXiv:2605.28925 [quant-ph]
[34] Albert V V and Jiang L 2014 *Phys. Rev. A* **89** 022118
[35] Gaiotto D, Kapustin A, Seiberg N, and Willett B 2015 *J. High Energ. Phys.* **02** 172
[36] Ji W and Wen X G 2020 *Phys. Rev. Res.* **2** 033417
[37] Kadanoff L P and Ceva H 1971 *Phys. Rev. B* **3** 3918
[38] Levin M 2020 *Commun. Math. Phys.* **378** 1081
[39] After the completion of this work, we became aware that a similar definition based on the domain-wall correlator was proposed by Ma and Turzillo [16].
[40] Kramers H A and Wannier G H 1941 *Phys. Rev.* **60** 252
[41] Li L, Bi Z, and Cao W 2026 arXiv:2603.17282 [cond-mat.str-el]
[42] Anderson P 1973 *Mater. Res. Bull.* **8** 153
[43] Sachdev S 1992 *Phys. Rev. B* **45** 12377
[44] Wen X G 2002 *Phys. Rev. B* **65** 165113
[45] Savary L and Balents L 2017 *Rep. Prog. Phys.* **80** 016502
[46] Barkeshli M, Bonderson P, Cheng M, and Wang Z 2019 *Phys. Rev. B* **100** 115147
[47] Chen X 2017 *Rev. Phys.* **2** 3
[48] Lu S and Lu Y M 2024 *Phys. Rev. B* **110** L100401
[49] Wang C Y, Zhou T G, Zhou Y N, and Zhang P 2024 *Phys. Rev. Lett.* **133** 083402
[50] Chen B B, Tu H H, Meng Z Y, and Cheng M 2022 *Phys. Rev. B* **106** 094415
[51] Huang Z M, Sun X Q, and Diehl S 2022 *Phys. Rev. B* **106** 245204
[52] Cai K L and Cheng M 2025 *Phys. Rev. B* **111** 205104
[53] Liu Z X, Gu Z C, and Wen X G 2014 *Phys. Rev. Lett.* **113** 267206
[54] Jiang W, Chen B B, Liu Z H, Rong J, and Assaad F F 2023 *SciPost Phys.* **15** 082
[55] Cai K L and Cheng M 2025 *Phys. Rev. B* **112** 155123
[56] Mao L, Zhai H, and Yang F 2025 *Chin. Phys. Lett.* **42** 067401
[57] Huang Z M and Diehl S 2025 *Phys. Rev. Res.* **7** 033028
[58] Huang Z M and Diehl S 2025 *Phys. Rev. Lett.* **134** 053002
[59] Ho W W, Cincio L, Moradi H, Gaiotto D, and Vidal G 2015 *Phys. Rev. B* **91** 125119
[60] Fradkin E and Shenker S H 1979 *Phys. Rev. D* **19** 3682
[61] Haegeman J, Zauner V, Schuch N, and Verstraete F 2015 *Nat. Commun.* **6** 8284
[62] Han T H, Helton J S, Chu S, Nocera D G, Rodriguez-Rivera J A, Broholm C, and Lee Y S 2012 *Nature* **492** 406
[63] Zhang C, Xu Y, Zhang J H, Xu C, Bi Z, and Luo Z X 2025 *Phys. Rev. B* **111** 115137
[64] Kong L, Lan T, Wen X G, Zhang Z H, and Zheng H 2020 *Phys. Rev. Res.* **2** 043086